

Fermi National Accelerator Laboratory

FERMILAB-Conf-96/370

Reliability of α_1 and α_2 from Lattice Codes

K.Y. Ng

*Fermi National Accelerator Laboratory
P.O. Box 500, Batavia, Illinois 60510*

October 1996

*Proceedings of Snowmass 96: New Directions for High Energy Physics, Snowmass, Colorado,
June 25-July 12, 1996.*

Disclaimer

This report was prepared as an account of work sponsored by an agency of the United States Government. Neither the United States Government nor any agency thereof, nor any of their employees, makes any warranty, express or implied, or assumes any legal liability or responsibility for the accuracy, completeness or usefulness of any information, apparatus, product or process disclosed, or represents that its use would not infringe privately owned rights. Reference herein to any specific commercial product, process or service by trade name, trademark, manufacturer or otherwise, does not necessarily constitute or imply its endorsement, recommendation or favoring by the United States Government or any agency thereof. The views and opinions of authors expressed herein do not necessarily state or reflect those of the United States Government or any agency thereof.

Distribution

Approved for public release: further dissemination unlimited.

Reliability of α_1 and α_2 from Lattice Codes

K. Y. Ng

Fermi National Accelerator Laboratory,* P.O. Box 500, Batavia, IL 60510

ABSTRACT

Whether the higher-order terms in the momentum-compaction factor, α_1 and α_2 , can be obtained reliably from lattice codes is an important issue for some quasi-isochronous rings. A FODO lattice consisting of thin quadrupoles, dipoles filling all spaces, and two families of thin sextupoles is solved and α_1 and α_2 are derived analytically. We find accurate agreement with SYNCH for α_1 but not α_2 . Possible error in SYNCH is examined. Some methods of measurement of α_1 and α_2 are discussed.

I. INTRODUCTION

The high luminosity of the recently proposed 2 TeV-2 TeV muon-muon collider [1] calls for a collider ring of circumference $C_0 \sim 8000$ m with an rms bunch length of 3 mm (10 ps) and rms momentum spread of 0.15%. The short bunch length, as well as a reasonable rf voltage, limits the slippage factor of the collider to $|\eta| \lesssim 1 \times 10^{-6}$ for every particle in the muon bunch [2, 3]. This implies that the spread of η as a function of momentum offset δ needs to be less than $\sim 1 \times 10^{-6}$ also.

The slippage factor and closed-orbit length C of an off-momentum particle can be expanded as power series in momentum offset δ ,

$$\eta = \eta_0 + \eta_1\delta + \eta_2\delta^2 + \dots, \quad (1.1)$$

$$C = C_0(1 + \alpha_0\delta + \alpha_1\delta^2 + \alpha_2\delta^3 + \dots), \quad (1.2)$$

where α_i is the i th-order term of the momentum-compaction factor. For a 2 TeV muon having $\gamma^{-2} = 2.73 \times 10^{-9}$, which is very much less than the required $|\eta|$, it can be readily shown that $\eta_1 \approx \alpha_1$ and $\eta_2 \approx \alpha_2$ [3].

With so tiny a value of $|\eta_0|$, the contributions of the higher-order term of the momentum-compaction factor can bring in a large spread in the slippage factor. To satisfy the zeroth-order momentum-compaction factor α_0 , the collider lattice can be designed rather easily, for example, using flexible momentum-compaction modules [4]. The first order α_1 brings in momentum asymmetry of the rf bucket and will lead to severe longitudinal head-tail instability [5]. Fortunately this instability can be avoided by reducing or eliminating the contribution of α_1 through the deployment of sextupoles [3]. However, the second order term α_2 will come into play.

For lattice structure that is as complicated as the flexible momentum-compaction module, analytic computations of α_1 and α_2 are almost impossible. The other design tool that we can rely on will be lattice codes such as the more common SYNCH [6] and MAD [7]. An obvious important question to ask is how reliable are these code-generated results, when higher orders of the momentum-compaction factor are concerned.

In this paper, we look into a FODO lattice consisting of thin quadrupoles, dipoles filling all spaces, and two families of sextupoles. When the exact solution is compared with the results from SYNCH, we find that SYNCH does not provide the correct α_2 . The source of error is investigated in Section III, and some possible ways to measure α_2 experimentally are discussed in Section IV. Section V is devoted to remarks and conclusions.

II. SIMPLIFIED FODO LATTICE

A. Momentum-Compaction Factor

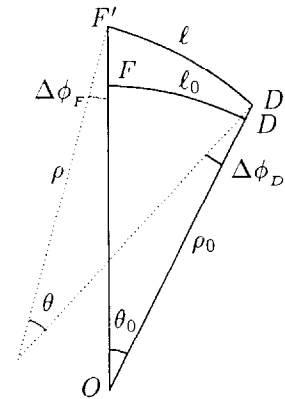


Figure 1: A FODO half cell with thin F- and D-quadrupoles and a dipole filling all spaces.

A simplified FODO lattice with only thin quadrupoles and with dipoles filling all spaces is soluble analytically [8]. Consider a half cell shown in Fig. 1. The half F-quadrupole is at FF' while the half D-quadrupole is at DD' . In between lies the dipole of bend angle θ_0 . The designed orbit in the half cell is the arc FD and is of length $\ell_0 = \rho_0\theta_0$ with radius of curvature ρ_0 , while the off-momentum closed orbit corresponding to δ is the arc $F'D'$ and is of length ℓ , radius of curvature ρ , and bend angle $\theta = \ell/\rho$. Passing through the thin half F-quadrupole, the off-momentum orbit acquires, according to the bending due to the Lorentz force, an angular change of

$$\Delta\phi_F = \frac{\delta}{1+\delta} \int ds \frac{B'\hat{D}\delta}{B_0\rho_0} = \frac{S\hat{D}}{\ell_0} \frac{\delta}{1+\delta}, \quad (2.1)$$

where

$$S = \ell_0 \left| \int ds \frac{B'}{B_0\rho_0} \right| \quad (2.2)$$

is the integrated strength of the quadrupole and B' the field gradient. The off-momentum orbit then turns through an angle θ inside the dipole and another

$$\Delta\phi_D = -\frac{S\hat{D}}{\ell_0} \frac{\delta}{1+\delta} \quad (2.3)$$

* Operated by the Universities Research Association, Inc., under contract with the U.S. Department of Energy.

through the half D-quadrupole to complete the half cell. In the above, \hat{D} and \check{D} represent the values of the dispersion function at the F- and D-quadrupoles, respectively. The total angle turned is obviously θ_0 . Therefore,

$$\theta = \theta_0 - \frac{S\delta}{1+\delta} \frac{\hat{D}-\check{D}}{\ell_0}. \quad (2.4)$$

Since the two orbits are in the same dipole field, their radii of curvature are related by $\rho = \rho_0(1+\delta)$. Combining Eqs. (2.4) and (2.5), we have for the two orbit lengths exactly

$$\ell = \ell_0 \left[1 + \delta \left(1 - \frac{S}{\theta_0} \frac{\hat{D}-\check{D}}{\ell_0} \right) \right]. \quad (2.5)$$

We can also include two families of half thin sextupoles of strengths

$$S_F = \int d\ell \frac{B''_{S_F}}{2B_0\rho_0} \quad S_D = \int d\ell \frac{B''_{S_D}}{2B_0\rho_0}, \quad (2.6)$$

placed, respectively, on each side of the F- and D-quadrupoles. The angle the off-momentum orbit turns at the half F-quadrupole and F-sextupole will change from Eq. (2.1) to

$$\Delta\phi_F = \frac{S\hat{D}\delta}{1+\delta} + \frac{S_F\hat{D}^2\delta^2}{1+\delta}. \quad (2.7)$$

Similarly, $\Delta\phi_D$ of Eq. (2.2) will change to

$$\Delta\phi_D = -\frac{S\check{D}\delta}{1+\delta} + \frac{S_D\check{D}^2\delta^2}{1+\delta}. \quad (2.8)$$

Equation (2.5) should also be changed accordingly. Note that the ℓ_0 has been removed since we have simplified the notations by measuring all lengths in terms of it.

With the expansions

$$\hat{D} = \hat{D}_0 + \hat{D}_1\delta + \hat{D}_2\delta^2 + \mathcal{O}(\delta^3), \quad (2.9)$$

$$\check{D} = \check{D}_0 + \check{D}_1\delta + \check{D}_2\delta^2 + \mathcal{O}(\delta^3), \quad (2.10)$$

for the dispersion function D , and Eq. (1.2) for the orbit length C , we arrive at each order of the momentum-compaction factor,

$$\begin{aligned} \alpha_0 &= 1 - \frac{S(\hat{D}_0 - \check{D}_0)}{\theta_0}, \\ \alpha_1 &= -\frac{S(\hat{D}_1 - \check{D}_1)}{\theta_0} - \frac{S_F\hat{D}_0^2}{\theta_0} - \frac{S_D\check{D}_0^2}{\theta_0}, \\ \alpha_2 &= -\frac{S(\hat{D}_2 - \check{D}_2)}{\theta_0} - \frac{2S_F\hat{D}_0\hat{D}_1}{\theta_0} - \frac{2S_D\check{D}_0\check{D}_1}{\theta_0}, \end{aligned} \quad (2.11)$$

which are exact to all orders of θ_0 .

B. A Geometric Solution

The off-momentum closed orbit $F'D'$ is an arc of a circle with radius $\rho = \rho_0(1+\delta)$. The equation of the arc contains only two constants plus \hat{D} and \check{D} . However, this arc is constrained by its positions and slopes at the dipole's entrance and exit. Therefore the two constants together with \hat{D} and \check{D} can be determined.

Consider OF' of Fig. 1 as the y -axis and O the origin. The x -axis is on the dipole side of OF' . The point F' is $(0, \rho_0 + \hat{D}\delta)$

and the arc $F'D'$ is at an angle $\Delta\phi_F$ given by Eq. (2.7). The equation of the arc $F'D'$ is therefore given by

$$\left[x + \rho \sin \Delta\phi_F \right]^2 + \left[y - \rho_0 - \hat{D}\delta + \rho \cos \Delta\phi_F \right]^2 = \rho^2. \quad (2.12)$$

Now rotate the x - and y -axes by an angle $\frac{1}{2}\theta_0$ so that the new y -axis passes through the center of the dipole. In terms of the new axes, the equation of the circular arc becomes

$$\begin{aligned} \left[x \cos \frac{\theta_0}{2} + y \sin \frac{\theta_0}{2} + \rho \sin \Delta\phi_F \right]^2 + \\ \left[-x \sin \frac{\theta_0}{2} + y \cos \frac{\theta_0}{2} - \rho_0 - \hat{D}\delta + \rho \cos \Delta\phi_F \right]^2 = \rho^2. \end{aligned} \quad (2.13)$$

We can also start with OD' as the y -axis. The angle at D' is now $\Delta\phi_D$ as given by Eq. (2.8). The axes are then rotated in the opposite direction by $\frac{1}{2}\theta_0$ so the the equation of the arc $F'D'$ becomes

$$\begin{aligned} \left[x \cos \frac{\theta_0}{2} - y \sin \frac{\theta_0}{2} + \rho \sin \Delta\phi_D \right]^2 + \\ \left[x \sin \frac{\theta_0}{2} + y \cos \frac{\theta_0}{2} - \rho_0 - \check{D}\delta + \rho \cos \Delta\phi_D \right]^2 = \rho^2. \end{aligned} \quad (2.14)$$

Equations (2.13) and (2.14) are exactly the same because they describe the same arc $F'D'$. By equating coefficients, we obtain with $t = \tan \frac{1}{2}\theta_0$,

$$\begin{aligned} \rho \sin \Delta\phi_F - \left[\rho \cos \Delta\phi_F - \hat{D}\delta - \rho_0 \right] t = \\ \rho \sin \Delta\phi_D + \left[\rho \cos \Delta\phi_D - \check{D}\delta - \rho_0 \right] t, \end{aligned} \quad (2.15)$$

$$\begin{aligned} t\rho \sin \Delta\phi_F + \left[\rho \cos \Delta\phi_F - \hat{D}\delta \right] = \\ -t\rho \sin \Delta\phi_D + \left[\rho \cos \Delta\phi_D - \check{D}\delta \right] t. \end{aligned} \quad (2.16)$$

The other relations are redundant. Thus, we can solve for \hat{D} and \check{D} in terms of θ_0 and δ exactly. Since we are interested in solution up to the second order in δ only, Eqs. (2.15) and (2.16) can be expanded and simplified. We then obtain for the zeroth order in δ ,

$$\begin{pmatrix} 1 & -t \\ t & 1 \end{pmatrix} \begin{pmatrix} S\hat{D}_0 \\ 1 - \theta_0\hat{D}_0 \end{pmatrix} = \begin{pmatrix} 1 & t \\ -t & 1 \end{pmatrix} \begin{pmatrix} S\check{D}_0 \\ 1 - \theta_0\check{D}_0 \end{pmatrix}, \quad (2.17)$$

for the first order in δ ,

$$\begin{aligned} \begin{pmatrix} 1 & -t \\ t & 1 \end{pmatrix} \begin{pmatrix} S\hat{D}_1 + S_F\hat{D}_0^2 \\ -\frac{1}{2}S^2\hat{D}_0^2 - \theta_0\hat{D}_1 \end{pmatrix} = \\ \begin{pmatrix} 1 & t \\ -t & 1 \end{pmatrix} \begin{pmatrix} S\check{D}_1 - S_D\check{D}_0^2 \\ -\frac{1}{2}S^2\check{D}_0^2 - \theta_0\check{D}_1 \end{pmatrix}, \end{aligned} \quad (2.18)$$

and for the second order in δ ,

$$\begin{pmatrix} 1 & -t \\ t & 1 \end{pmatrix} \begin{pmatrix} S\hat{D}_2 - \frac{1}{6}S^3\hat{D}_0^3 + 2S_F\hat{D}_0\hat{D}_1 \\ \frac{1}{2}S^2\hat{D}_0^2 - S^2\hat{D}_0\hat{D}_1 - \theta_0\hat{D}_0 - SS_F\hat{D}_0^3 \end{pmatrix} =$$

$$\begin{pmatrix} 1 & t \\ -t & 1 \end{pmatrix} \begin{pmatrix} S\check{D}_2 - \frac{1}{6}S^3\check{D}_0^3 - 2S_D\check{D}_0\check{D}_1 \\ \frac{1}{2}S^2\check{D}_0^2 - S^2\check{D}_0\check{D}_1 - \theta_0\check{D}_0 + SS_D\check{D}_0^3 \end{pmatrix}. \quad (2.19)$$

Solving Eq. (2.17), we obtain

$$\hat{D}_0, \check{D}_0 = \frac{\theta_0 \pm St}{S^2 + \theta_0^2}, \quad (2.20)$$

which are the usual expressions for the dispersions at the F- and D-quadrupoles of a FODO cell. The zeroth order of the momentum-compaction factor is, according to Eq. (2.11),

$$\alpha_0 = 1 - \frac{2S^2t}{\theta_0(S^2 + \theta_0^2)}. \quad (2.21)$$

Solving Eq. (2.18), we obtain the first order dispersion,

$$\begin{aligned} \hat{D}_1 = & -\frac{S^2\hat{D}_0^2(St^2 + 2\theta_0t - S)}{4t(S^2 + \theta_0^2)} - \frac{S^3\check{D}_0^2(1+t^2)}{4t(S^2 + \theta_0^2)} \\ & - \frac{S_F\hat{D}_0^2(2St - \theta_0t^2 + \theta_0)}{2t(S^2 + \theta_0^2)} - \frac{S_D\check{D}_0^2\theta_0(1+t^2)}{2t(S^2 + \theta_0^2)}, \end{aligned} \quad (2.22)$$

$$\begin{aligned} \check{D}_1 = & \frac{S^3\hat{D}_0^2(1+t^2)}{4t(S^2 + \theta_0^2)} - \frac{S^2\check{D}_0^2(2\theta_0t + S - St^2)}{4t(S^2 + \theta_0^2)} \\ & - \frac{S_F\hat{D}_0^2\theta_0(1+t^2)}{2t(S^2 + \theta_0^2)} - \frac{S_D\check{D}_0^2(\theta_0 - 2St - \theta_0t^2)}{2t(S^2 + \theta_0^2)}. \end{aligned} \quad (2.23)$$

The first-order term of the momentum-compaction factor can now be obtained from Eq. (2.11). It can be simplified to

$$\alpha_1 = -\frac{S^4t(S^2t^2 + 3\theta_0^2)}{\theta_0(S^2 + \theta_0^2)^3} - (S_F\hat{D}_0^3 + S_D\check{D}_0^3). \quad (2.24)$$

We see from Eq. (2.24) that α_1 can be reduced or eliminated by suitable deployment of sextupoles.

In the situation of a very large ring where $\theta_0 \ll S$, the above equations reduce to

$$\alpha_0 \rightarrow \frac{\theta_0^2}{S^2} \left(1 - \frac{S^2}{12}\right), \quad (2.25)$$

$$\alpha_1 \rightarrow \frac{3\theta_0^2}{2S^2} \left(1 + \frac{S^2}{12}\right) - (S_F\hat{D}_0^3 + S_D\check{D}_0^3). \quad (2.26)$$

Solution of Eq. (2.19) gives

$$\begin{aligned} \hat{D}_2 - \check{D}_2 = & \frac{1}{6}S^3\hat{D}_0^3\frac{S - t\theta_0}{S^2 + \theta_0^2} - \frac{1}{6}S^3\check{D}_0^3\frac{S + t\theta_0}{S^2 + \theta_0^2} \\ & + \frac{1}{2}S^2(\hat{D}_0^3 - \check{D}_0^3) - S^2(\hat{D}_0^2\hat{D}_1 - \check{D}_0^2\check{D}_1) \\ & - 2S_F\hat{D}_0\hat{D}_1\frac{S - t\theta_0}{S^2 + \theta_0^2} - 2S_D\check{D}_0\check{D}_1\frac{S + t\theta_0}{S^2 + \theta_0^2} \\ & - S(S_F\hat{D}_0^4 + S_D\check{D}_0^4). \end{aligned} \quad (2.27)$$

Substituting into Eq. (2.11) will give α_2 . As is seen in Eqs. (2.22) and (2.23), \hat{D}_1 and \check{D}_1 are linear in S_F and S_D , α_2 will have quadratic terms in the sextupole strengths, indicating that the sextupoles talk to each other in their contributions to the second-order term of the momentum-compaction factor.

In the large ring approximation, $\theta_0^2 \ll 1$, Eq. (2.27) can be simplified considerably. In the absence of sextupoles, we obtain

$$\alpha_2 \rightarrow -\frac{\theta_0^2}{6} \left(1 + \frac{35\theta_0^2}{S^4}\right), \quad (2.28)$$

where we have included the $\mathcal{O}[(\theta/S)^4]$ term because the $\mathcal{O}[(\theta/S)^2]$ term happens to have canceled out. Note that α_0 , α_1 and α_2 are all of order θ_0^2 . Therefore, it may be more convenient to quote their ratios instead; i.e.,

$$\frac{\alpha_1}{\alpha_0} \rightarrow \frac{3}{2} \left(\frac{1 + \frac{1}{12}S^2}{1 - \frac{1}{12}S^2}\right), \quad \frac{\alpha_2}{\alpha_0} \rightarrow -\frac{S^2}{6} \left(\frac{1 + \frac{35\theta_0^2}{S^4}}{1 - \frac{1}{12}S^2}\right). \quad (2.29)$$

C. Comparison with SYNCH and MAD

A numerical comparison of α_2 had been made in Ref. 8 with the theoretical results of a simplified FODO lattice with only thin quadrupoles and with dipoles filling all spaces. A ring consisting of 150 equal FODO cells and another one consisting of 15 equal FODO cells were considered. The half-cell length was fixed at $\ell_0 = 2\pi$ m, and the half quadrupole strength was varied from $S = 0.020$ to 0.999. The first-order momentum-compaction factor α_1 was extracted from SYNCH in each case and was compared with the analytic expression derived above. The agreements had been excellent, up to at least 3 significant figures. A comparison had also been made with the addition of two families of sextupoles. The agreement had also been excellent, thus verifying the validity of Eq. (2.24). This does not, however, exclude the possibility of a disagreement of α_1 with lattice consisting of thick quadrupoles and thick sextupoles. This is because the exact integration of the particle trajectory inside a quadrupole or sextupole is tedious and time consuming, and lattice codes usually resort to approximations.

Here, we continue to use a lattice consisting of 150 equal FODO cells to study the second-order term of the momentum-compaction factor α_2 . The half sextupole strength is chosen to be $S = \frac{1}{2}$ or a phase advance of $\mu = 2\sin^{-1}\frac{1}{2} = \frac{\pi}{3}$.

What we obtain from SYNCH are the transition gammas γ_t 's at various momentum offsets, with γ_t defined as

$$\gamma_t^{-2} = \frac{\delta}{C} \frac{dC}{d\delta}, \quad (2.30)$$

which can be expanded as a power series in momentum offset δ ,

$$\gamma_t^{-2} = a_0 + a_1\delta + a_2\delta^2 + \dots \quad (2.31)$$

Comparing with the power expansion of the closed-orbit length in Eq. (1.2), the various orders of the momentum-compaction factor are obtained:

$$\begin{aligned} \alpha_0 &= a_0, \\ 2\alpha_1 &= a_1 - a_0 + a_0^2, \\ 3\alpha_2 &= a_2 - a_1 + a_0 + \frac{3}{2}a_0a_1 - \frac{3}{2}a_0^2 + \frac{1}{2}a_0^3. \end{aligned} \quad (2.32)$$

When the γ_t^{-2} 's from SYNCH for momentum offset varying between ± 0.0004 are fitted by a polynomial of degree two as indicated in Eq. (2.31), we obtain the three coefficients: $a_0 = 0.00171503$, $a_1 = 0.00705748$, and $a_2 = 0.00853026$. The corresponding orders of the momentum-compaction factor are extracted according to Eq. (2.32) and are listed in Table I along with the analytically computed values of Eq. (3.11). The results of MAD were obtained in exactly the same way. Notice that the

approximate expressions of Eqs. (2.25), (2.26), and (2.28) for the α 's are pretty accurate. It is obvious that α_2 has not been given correctly by SYNCH and MAD. We also tried to fit the γ_t^{-2} 's obtained from the codes to polynomials of degree 3; the first three α 's do not change in their first 4 significant figures.

Table I: Comparison of SYNCH and MAD with theoretical results for the simplified FODO lattice.

	SYNCH	MAD	Theory
α_0	0.00171503	0.00171503	0.00171518
α_1	0.00267272	0.00267421	0.00267273
α_2	0.00105371	0.00064879	-0.00009099

III. SYNCH AND MAD COMPUTATIONS

In a lattice code, the usual way to compute γ_t for an off-momentum particle is (1) to compute the off-momentum closed orbit and (2) to compute the derivative in Eq. (2.30) by offsetting the momentum slightly. The second step seems to be fine, because both SYNCH and MAD give us the correct γ_t for the on-momentum particle.

As for the off-momentum closed orbit, SYNCH [6] first tracks an initial "first guess" particle state vector V_0 through one complete revolution so as to produce a new state vector V_1 . These state vectors are 7-element vectors; for example,

$$V = (x, x', y, y', -ds, \delta, 1), \quad (3.1)$$

where the first 4 entries are for the horizontal and vertical deviations and slopes, the 5th denotes the shortening in orbit length, the 6th momentum offset, and the 7th is reserved for misalignment calculation. The transfer matrices of the ring's elements are then linearized about this initial single-turn trajectory, generating new transfer matrices, R , and a linearized single-turn transfer matrix $T = R_N R_{N-1} \cdots R_2 R_1$.

One may now track a particle vector X_0 in a small neighborhood of V_0 so that $X_0 = V_0 + Z_0$. After one revolution, this vector becomes $X_1 = V_1 + Z_1$, where $Z_1 = TZ_0$. If X_0 is a closed orbit, we must have $X_0 = X_1$, or

$$X_0 = V_0 + Z_0 = V_1 + Z_1. \quad (3.2)$$

Therefore,

$$X_0 = V_1 + TZ_0 = V_1 + T(X_0 - V_0), \quad (3.3)$$

or the closed orbit is

$$X_0 = V_0 + (I - T)^{-1}(V_1 - V_0), \quad (3.4)$$

where I is the identity matrix. Then X_0 is used as the new guess vector, and the iterations are repeated. The exact off-momentum closed orbit should then be available.

Let us examine this closed orbit for the simplified 150-cell FODO lattice discussed above. We read out the maximum and minimum dispersions from the SYNCH and MAD outputs for different momentum offsets and fit polynomials of degree 3 to extract the different orders of the dispersion. The results are listed in Table II. Some numbers from MAD are omitted, because the \hat{D} 's are given to 3 figures only and are not accurate enough to do a polynomial fitting. We see that only the zeroth orders agree with theory.

Using the SYNCH results of \hat{D}_1 and \check{D}_1 , we cannot arrive at the correct value of α_1 via Eq. (2.11) as listed in Table II. In fact, SYNCH computes γ_t separately using the derivative $dC/d\delta$ according to Eq. (2.30). Since α_1 from SYNCH agrees with theory (see Table I), we can conclude that the $\hat{D}_1 - \check{D}_1$ from analytic calculation is correct and those from SYNCH and MAD are incorrect. It is not impossible that there will be error in SYNCH when the off-momentum closed orbit is computed. In fact, it is non-trivial to propagate an off-momentum particle through lattice elements having magnet field

$$B = B_0 + B'|_0 x + \frac{1}{2} B''|_0 x^2 + \cdots = B_0 \rho_0 \left[\frac{1}{\rho_0} + Kx \right], \quad (3.5)$$

where x is the horizontal deviation from the designed orbit. Although the zeroth and first order differential equations for x are simple, the exact one is very complicated [8],

$$x'' = \frac{x'^2}{\rho_0(1+x/\rho_0)} + \left(1 + \frac{x}{\rho_0}\right) \left[1 + \frac{x'^2}{(1+x/\rho_0)^2}\right] \times \left\{ \frac{1}{\rho_0} - \frac{1}{1+\delta} \left[1 + \frac{x'^2}{(1+x/\rho_0)^2}\right]^{\frac{1}{2}} \left(1 + \frac{x}{\rho_0}\right) \left(\frac{1}{\rho_0} + Kx\right) \right\}.$$

Since only the zeroth order off-momentum closed orbit is correct in SYNCH, γ_t^{-2} computed using Eq. (2.30) can only be correct to the first order in δ . This explains why α_2 has been computed wrongly by SYNCH and MAD.

Table II: Comparison of SYNCH and MAD with theoretical results for the dispersion function.

	SYNCH	MAD	Theory
\check{D}_0	0.65683 m	0.65683 m	0.65683 m
\hat{D}_0	0.39409 m	0.394 m	0.39409 m
\hat{D}_1	1.70435 m	1.70236 m	0.52278 m
\check{D}_1	1.44461 m	1.463 m	0.52348 m
\hat{D}_2	4.61014 m	0.98741 m	
\check{D}_2	4.88449 m		
$\hat{D}_2 - \check{D}_2$	-0.27435 m		0.00002395 m

IV. MEASUREMENT OF α_1 AND α_2

Since α_2 is not predictable with lattice codes and is difficult to calculate theoretically for a real accelerator consisting of, for example, low-beta insertions, flexible momentum-compaction modules, and dispersion suppressors, we must resort to measurements [9]. The slippage factor can be inferred by the synchrotron tune of a particle in an off-momentum orbit. This can be done by altering the rf frequency from f_{rf} by an amount Δf_{rf} so that the synchronous particle is in a different closed orbit of length $C_0 + \Delta C$ at a momentum $p_0 + \Delta p = p_0(1 + \delta_0)$. The phase equation per turn for a particle with momentum offset δ is

$$\frac{d\Delta\phi}{dn} = 2\pi\eta(\delta)(\delta - \delta_0). \quad (4.1)$$

This is because the synchronous particle which is at $\delta = \delta_0$ should have zero phase slip. With $\Delta\delta = \delta - \delta_0$, Eq. (4.1) can be rewritten as

$$\frac{d\Delta\phi}{dn} = 2\pi \left[\eta(\delta_0)\Delta\delta + \eta'(\delta_0)\Delta\delta^2 + \frac{1}{2}\eta''(\delta_0)\Delta\delta^3 + \dots \right]. \quad (4.2)$$

Thus the synchrotron tune, $\nu_s = \nu_{s0}\sqrt{\eta(\delta_0)/\eta_0}$, becomes

$$\nu_s = \nu_{s0} \left[1 + \frac{\eta_1}{2\eta_0}\delta_0 + \left(\frac{\eta_2}{2\eta_0} - \frac{\eta_1^2}{8\eta_0^2} \right) \delta_0^2 + \dots \right], \quad (4.3)$$

where ν_{s0} is the synchrotron tune for the on-momentum particle when $\eta = \eta_0$, and the η_i 's with $i = 1, 2, \dots$ are the higher-order expansion terms of the slippage factor as given by Eq. (1.1). From Eq. (1.2), the momentum offset can be written in terms of the orbit-length offset,

$$\delta_0 = \frac{\Delta C}{\alpha_0 C_0} - \frac{\alpha_1}{\alpha_0} \left(\frac{\Delta C}{\alpha_0 C_0} \right)^2 + \dots. \quad (4.4)$$

Since $\Delta C/C_0 = -\Delta f_{rf}/f_{rf}$, substituting Eq. (4.4) into Eq. (4.3), we arrive at

$$\nu_s = \nu_{s0} \left[1 - \frac{\eta_1}{\eta_0^2} \left(\frac{\Delta f_{rf}}{f_{rf}} \right) - \left(\frac{5\eta_1^2}{8\eta_0^4} - \frac{\eta_2}{2\eta_0^3} \right) \left(\frac{\Delta f_{rf}}{f_{rf}} \right)^2 + \dots \right], \quad (4.5)$$

where we have used $\eta_0 \approx \alpha_0$ and $\eta_1 \approx \alpha_1$.

The maximum momentum spread of the designed muon bunch is $\delta_{\max} = 0.003$ and $\eta \approx 1 \times 10^{-6}$. Therefore a variation of the rf frequency by $\Delta f_{rf}/f_{rf} \approx 3 \times 10^{-9}$ will be required. Since the figure of merit of a superconducting cavity can easily reach $Q = 1 \times 10^9$, such an rf frequency variation should be possible.

A low-intensity proton bunch with small momentum spread is injected into the muon collider for the measurement. The on-momentum synchrotron tune will give η_0 . The higher orders η_1 and η_2 can be inferred by measuring the synchrotron tune as a function of $\Delta f_{rf}/f_{rf}$. If no asymmetric variation of the synchrotron tune is observed when $\Delta f_{rf}/f_{rf}$ varies between $\pm 3 \times 10^{-9}$, we can conclude that the η_1 contribution is insignificant in this collider lattice. Furthermore, if the synchrotron tune remains flat during the variation of $\Delta f_{rf}/f_{rf}$, the η_2 contribution is also insignificant. The bucket will then be η_0 -dominated. However, if we see a symmetric parabolic dependency of ν_s versus $\Delta f_{rf}/f_{rf}$, we can tune the machine so that η_0 becomes zero. The bucket will then be η_2 -dominated and the magnitude of η_2 can be determined easily.

Strictly speaking, Eqs. (4.3) to (4.4) are not valid when the contribution η_0 is small. Under that situation, we can write

$$\nu_s = \left(\frac{heV}{2\pi\beta^2 E} \right)^{\frac{1}{2}} [\eta_0 + \eta_1\delta_0 + \eta_2\delta_0^2]^{\frac{1}{2}}, \quad (4.6)$$

and solve for δ_0 in terms of $\Delta C/C_0$ exactly from Eq. (1.2). Here, h is the rf harmonic, V the rf voltage, E the energy of the synchronous particle and β its velocity divided by the velocity of light. After substituting the result into Eq. (4.6), we will then obtain ν_s in terms of $\Delta f_{rf}/f_{rf}$ which is valid for all values of η_0 , η_1 , and η_2 . For example, when the contribution of η_2 overshadows those of η_0 and η_1 , we have,

$$\nu_s = \left(\frac{heV}{2\pi\beta^2 E} \right)^{\frac{1}{2}} \eta_2^{\frac{1}{3}} \left| \frac{\Delta f_{rf}}{f_{rf}} \right|^{\frac{2}{3}}, \quad (4.7)$$

except when $\Delta f_{rf}/f_{rf}$ is very close to zero. Similarly, for an asymmetric α -like bucket [10],

$$\nu_s = \left(\frac{heV}{2\pi\beta^2 E} \right)^{\frac{1}{2}} \left[\frac{\eta_0}{2} + \left(\frac{\eta_0^2}{4} - \eta_1 \frac{\Delta f_{rf}}{f_{rf}} \right)^{\frac{1}{2}} \right]. \quad (4.8)$$

V. CONCLUSION

A simplified FODO lattice consisting of thin quadrupoles and sextupoles with dipoles filling all spaces has been solved and an analytic expression for α_2 has been presented. Comparison with the results of SYNCH gives agreement with α_1 but not α_2 .

We have examined the way SYNCH and MAD compute the transition gamma for off-momentum particles, which consists of computing the off-momentum closed orbit and then the γ_t around the closed orbit using a derivative. We have compared each order of the dispersion with theory and found that only the lowest order is accurate. The error appears to come from the inaccurate tracking of an off-momentum particle across a quadrupole and/or sextupole. With the closed orbit only accurate to first order in δ , it is obvious that SYNCH and MAD cannot provide the correct value for α_2 .

Some experimental measurements of α_1 and α_2 have been suggested. The method consists of offsetting the closed orbit of the synchronous particle by altering the rf frequency and measuring the change in synchrotron frequency. Since a superconducting cavity can have a figure of merit as high as $Q = 1 \times 10^9$, accurate measurements of α_1 and α_2 should be feasible.

VI. REFERENCES

- [1] The $\mu^+\mu^-$ Collider Collaboration, *Muon Muon Collider: A Feasibility Study*, 1996, Ed. J. Gallardo, p.326. Also published as Internal Lab. Notes: BNL-52503, Fermi Lab-Conf.-96/092, and LBNL-38946.
- [2] A. Garren, et al., *Design of the Muon Collider Lattice: Present Status*, to appear in Proc. San Francisco Workshop Physics of Muon Colliders, 1996.
- [3] K.Y. Ng, *The Quasi-Isochronous Buckets of the Muon Collider*, Fermilab Internal Report FN-648, 1996.
- [4] S.Y. Lee, K.Y. Ng, and D. Trbojevic, Phys. Rev.E, **48**, 3040-3048 (1993).
- [5] D. Boussard and T. Linnecar, Proc. 2nd European Particle Accelerator Conference, Nice, June 990, Ed. P. Martin and P. Mandrillon, p. 1560.
- [6] A.A. Garren, A.S. Kenney, E.D. Courant, and M.J. Syphers, *A User's Guide to SYNCH*, Fermilab Internal Note FN-420, 1985.
- [7] H. Grote and F.C. Iselin, *The MAD Program, Version 8.1, User's Reference Manual*, CERN Report CERN/SL/90-13(AP), 1990.
- [8] K. Ng, *Higher-order Momentum Compaction for a Simplified FODO Lattice and Comparison with SYNCH*, Fermilab Report FN-578, 1991.
- [9] D. Robin, H. Hama, and A. Nadji, *Experimental Results on Low Alpha Electron-Storage Rings*, Proc. Micro Bunches Workshop, Upton, NY, Sep. 28-30, 1995, Ed. E.B. Blum, M. Dienes, and J.B. Murphy, (AIP Conf. Proc. 367), p. 150; D. Robin, R. Alvis, A. Jackson, R. Holtzapple, and B. Podobedov, *Low Alpha Experiments at the ALS, ibib*, p. 181.
- [10] H. Hama, S. Takano, and G. Isoyama, Nucl. Inst. Meth. **A329**, 29 (1993).